TÜBİTAK

Turkish Journal of Medical Sciences

http://journals.tubitak.gov.tr/medical/

Research Article

Turk J Med Sci
(2013) 43: 775-781
© TÜBİTAK
doi:10.3906/sag-1206-32

Determination of mitochondrial fragmentation and autophagosome formation in C2C12 skeletal muscle cells

Saadet TÜRKSEVEN[1,*], Antonio ZORZANO[2,3,4]

[1]Department of Pharmacology, Faculty of Pharmacy, Ege University, Bornova, İzmir, Turkey
[2]Institute for Research in Biomedicine (IRB Barcelona), Barcelona, Spain
[3]Department of Biochemistry and Molecular Biology, Faculty of Biology, University of Barcelona, Barcelona, Spain
[4]Spanish Biomedical Research Centre in Diabetes and Associated Metabolic Disorders (CIBERDEM), Instituto de Salud Carlos III, Madrid, Spain

Received: 09.06.2012 • **Accepted:** 08.01.2013 • **Published Online:** 26.08.2013 • **Printed:** 20.09.2013

Aim: To investigate the effect of carbonyl cyanide 3-chlorophenylhydrazone (CCCP) on mitochondrial elimination in C2C12 skeletal muscle cells.

Materials and methods: C2C12 muscle cells stably expressing Mito-DsRed were treated with DMSO or CCCP at the doses of 10, 20, and 30 μM for 3, 6, and 24 h. After specific treatments, cells were fixed in 4% paraformaldehyde and immunocytochemistry assays were performed using appropriate antibodies to evaluate mitochondrial morphology and autophagosome formation. Total cell lysates were used for western blot assays.

Results: CCCP induces mitochondrial fragmentation in C2C12 cells. In response to a mitochondrial uncoupler, endogenous autophagosome formation is significantly increased ($P < 0.001$). Co-localization analyses of confocal images indicate that fragmented mitochondria undergo engulfment by autophagosomes.

Conclusion: The findings of this study will enhance our understanding of the mitophagic process in C2C12 skeletal muscle cells in order to identify molecular mechanisms governing removal of dysfunctional mitochondria.

Key words: Mitophagy, LC3, skeletal muscle cell

1. Introduction

Mitochondria are dynamic organelles that are constantly undergoing fission and fusion to adapt to changes in the cellular environment. The combination of fusion and fission is a quality-control mechanism of the mitochondrial network that maintains a healthy mitochondrial population and cellular homeostasis. Following depolarization, mitochondria do not undergo fusion and are targeted by mitochondria elimination systems in the cell (1–3).

Accumulation of depolarized mitochondria within the cells has been associated with oxidative damage and the development of several pathological conditions, such as neurodegenerative diseases, cardiovascular diseases, or diabetes (2–8). In mammalian cells, the dissipation of the mitochondrial membrane potential triggers the specific and selective removal of damaged mitochondria from the cell via autophagy, termed mitophagy (9,10). The selective removal of mitochondria by autophagic machinery includes formation of double-membrane vesicles, autophagosomes, which engulf mitochondria labeled for degradation and sequentially deliver the cargo to lysosomes (11). Formation of autophagosomes requires microtubule-associated protein-1 light chain 3 (LC3) lipidation. Phospholipid conjugated LC3 (LC3-II) is mainly localized on autophagosomes and autolysosomes (12). In this respect, LC3-II accumulation is a marker for the formation of autophagosomes (13). Removal of mitochondria by autophagic machinery also occurs during differentiation of some cells and is essential for the proper organ development (14). Several mitochondria localized proteins, such as BCL2/adenovirus E1B 19-kDa protein-interacting protein 3 (BNIP3) and Nix (also known as BNIP3L), have been implicated in the removal of damaged mitochondria (15,16) in mammals to date. PARK2, a gene encoding the E3 ubiquitin ligase Parkin, is the major cause of autosomal recessive Parkinson disease (17) and triggers

* Correspondence: saadet.turkseven@ege.edu.tr

the clearance of damaged mitochondria by translocating to the depolarized mitochondria (18,19).

Thus far, although several mitophagy regulators have been discovered, many questions still remain to be answered. Studies on cells with bioenergetically heterogeneous populations of mitochondria (due to carbonyl cyanide 3-chlorophenylhydrazone [CCCP]-induced damage) help to understand the regulation of mitophagy in different cell lines. In this study, we investigated mitochondrial depolarization and fragmentation, which is the primary signal for mitophagy, by using a pharmacological approach. C2C12 muscle cells were treated with the mitochondrial uncoupler CCCP at different time points and mitochondrial fragmentation was monitored by confocal microscopy. Since mitochondria are eliminated by autophagy machinery, we further checked LC3 formation as an autophagy marker. Our results clearly showed that CCCP induces mitochondrial fragmentation and depolarization, and massive endogenous LC3 formation was observed after mitochondrial depolarization. Co-localization analysis also showed that fragmented mitochondria undergo engulfment by autophagosomes, suggesting the mitophagic clearance of damaged mitochondria in C2C12 cells.

2. Materials and methods

2.1. Antibodies and reagents

The following primary antibodies were used: anti-LC3 (clone 5F10; Nanotools for immunofluorescence assay and MBL International for western blot) and antitubulin (Sigma). Antirabbit or antimouse horseradish peroxidase (HRP) conjugated secondary antibodies (Jackson ImmunoResearch) were used for western blot assays. A secondary antibody conjugated with Alexa Fluor 488 (Invitrogen) was used for immunofluorescence.

Cells were treated with dimethyl sulfoxide (DMSO) or CCCP as indicated in the text. All other reagents used in this study were obtained from Sigma.

2.2. Cell culture and treatments

C2C12 skeletal muscle cells stably expressing Mito-DsRed were maintained in Dulbecco's Modified Eagle Medium (DMEM, GIBCO) supplemented with 10% fetal bovine serum (FBS, GIBCO), 25 mM HEPES, penicillin (100 U/mL), and streptomycin (100 µg/mL). Cells were treated for various times with 10, 20, or 30 µM CCCP or DMSO as a control in order to determine the mitochondrial fragmentation and LC3 formation. After the treatments, cells were subjected to different assays.

2.3. Immunofluorescence assays

After specific treatments, cells were fixed in 4% paraformaldehyde and washed 3 times with phosphate buffered saline (PBS). Immunocytochemistry assays were performed using an antibody against LC3. Hoechst (1/2000; Molecular Probes) was used to label DNA. Cells were mounted in Mowiol (Sigma). Immunofluorescence microscopy of the cells was performed with a Leica TCS SP2 confocal scanning microscope (Leica Lasertechnik GmbH, Germany), adapted to an inverted LEICA DM IRE2 microscope to perform the sequential acquisition of multiple cellular staining. Samples were scanned using a 63 × 1.40 NA objective (oil) and a zoom ranging from 1 to 3.5 to analyze intracellular regions using the software LCS from Leica. The fluorochromes used (DAPI, Alexa Fluor 488, DsRed) were excited with 405 (UV), 488, and 561 laser lines, respectively. To avoid bleed-through effects (i.e. crosstalk of different fluorescence emission) in double or triple staining experiments, each dye was scanned independently. Moreover, we demonstrated that the green channel does not emit in the red channel by doing separate acquisitions, and by exciting in one wavelength (green, 488 nm) and acquiring images in the higher wavelength (red, 561 nm). The projection format was 1024 × 1024. Images were acquired from 10 to 20 optical sections. Figures were assembled from the TIFF and LEI files using open software ImageJ (author: Wayne Rasband, National Institute of Mental Health, Bethesda, Maryland, USA). The PDM is the product of the differences from the means (PDM = (red intensity – mean red intensity) × (green intensity – mean green intensity)) and it is calculated and normalized for each pixel of an image and expresses the degree of co-localization of 2 signals with a value varying from –1 to +1. A value of –1 represents maximal exclusion, negative values express asynchronous localization, positive values express synchronous localization (or co-localization), and +1 expresses maximal co-localization. On the images, pixels that did not co-localize (negative values of PDM) are represented with a blue intensity gradient, while co-localizing values are shown with a gradient of yellow. PDM images were calculated using the Image J ICA plugin (created by Tony Collins, McMaster University, Ontario, Canada) (20).

2.4. Western blot assays

Protein levels were visualized by immunoblotting with antibodies against LC3 and α-tubulin. LC3 is a very labile protein. In order to detect it by western blot, we had to follow a particular protocol. Cultured cells were lysed by addition of lysis buffer containing 50 mM Tris-HCl (pH 6.8), 10% (v/v) glycerol, 2% SDS, and a complete protease inhibitor cocktail (Roche). Immediately afterwards, samples were incubated for 5 min at 95 °C. The protein concentrations were then quantified by the Pierce method and the samples were stored at –20 °C or processed for western blot.

Briefly, 30 µg of lysate supernatant was separated by 15% SDS/polyacrylamide gel electrophoresis and

transferred to PVDF membranes (Millipore) using a wet transfer apparatus (Bio-Rad, USA). The membranes were incubated with 5% milk in a PBS (pH 7.4) and 0.1% Tween 20 (PBS-T) buffer at room temperature for 1 h. After washing with PBS-T, the membranes were incubated with antibodies against LC3 and α-tubulin at 4 °C overnight with constant shaking. The filters were washed 3 times with PBS-T and subsequently probed with HRP conjugated donkey antirabbit or antimouse IgG. Chemiluminescence detection was performed with an Amersham ECL detection kit according to the manufacturer's instructions.

2.5. Statistical analysis

The data are expressed as the mean ± standard error of the mean of the number of experiments (n). The statistical significance between the experimental groups was determined by a 2-tailed unpaired t-test. P-values of less than 0.05 were considered statistically significant.

3. Results

3.1. CCCP induces mitochondrial fragmentation in C2C12 skeletal muscle cells

C2C12 skeletal muscle cells are capable of differentiation and the number of mitochondria in these cells is abundant since the amount of mitochondria in the cells varies widely depending on the oxygen demand (21). In this study, to monitor mitochondria we used C2C12 skeletal muscle cells stably expressing Mito-DsRed. CCCP is a lipid-soluble weak acid and a known potent mitochondrial uncoupling agent that increases the proton permeability across the mitochondrial inner membranes and causes mitochondrial depolarization (18,22). In this study, our primary aim was to monitor the fragmentation of mitochondria upon CCCP treatment at different time points and doses. In C2C12 skeletal muscle cells treated with DMSO, mitochondria were highly elongated and fused with the network (Figures 1 and 2). After 10, 20, and 30 μM CCCP treatment for 3 h, mitochondria underwent marked structural changes. Elongated mitochondria completely disappeared, suggesting the induction of massive mitochondrial fragmentation (Figure 1). We also monitored the mitochondrial morphology after 6 h of CCCP treatment at the doses of 10, 20, and 30 μM (Figure 2). With the 30 μM dose, mitochondria were mainly localized around the perinuclear region, whereas 10 μM CCCP treatment caused dispersed fragmented mitochondria in the cytosol. Our confocal images clearly showed that CCCP-induced mitochondrial fragmentation is time- and dose-dependent, although a low dose and little time were sufficient to trigger mitochondrial uncoupling and fragmentation.

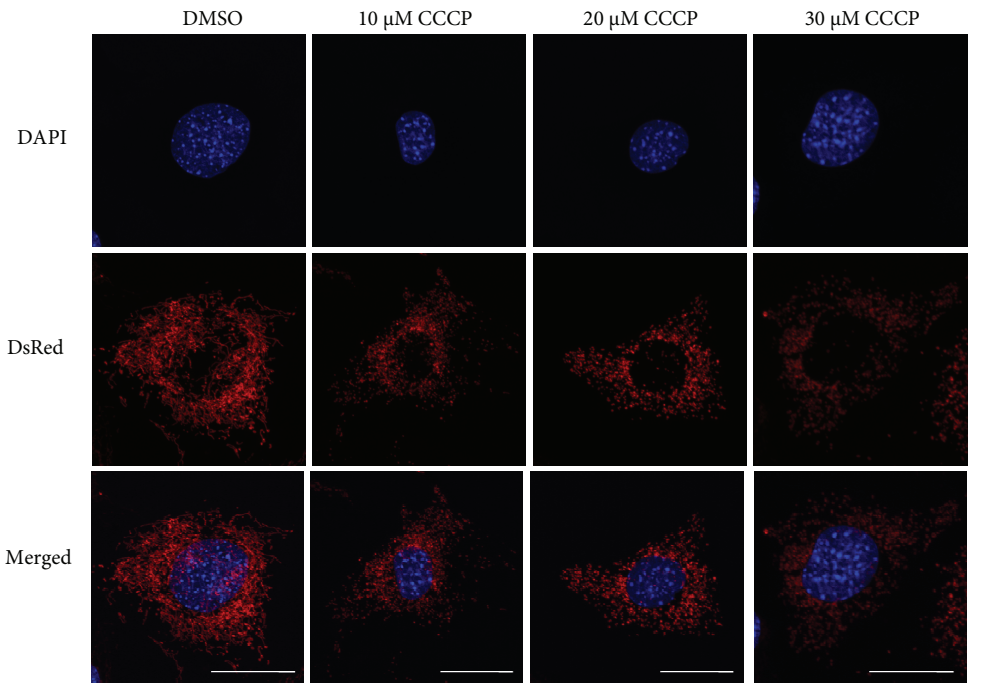

Figure 1. CCCP treatment for 3 h induces mitochondrial fragmentation. Confocal images of C2C12 skeletal muscle cells stably expressing Mito-DsRed treated with 10, 20, and 30 μM of CCCP for 3 h. Nuclei were stained with DAPI and are shown in blue. Mitochondria are shown in red. DAPI and DsRed were excited with 405 (UV) and 561 laser lines, respectively. Scale bars = 10 μm.

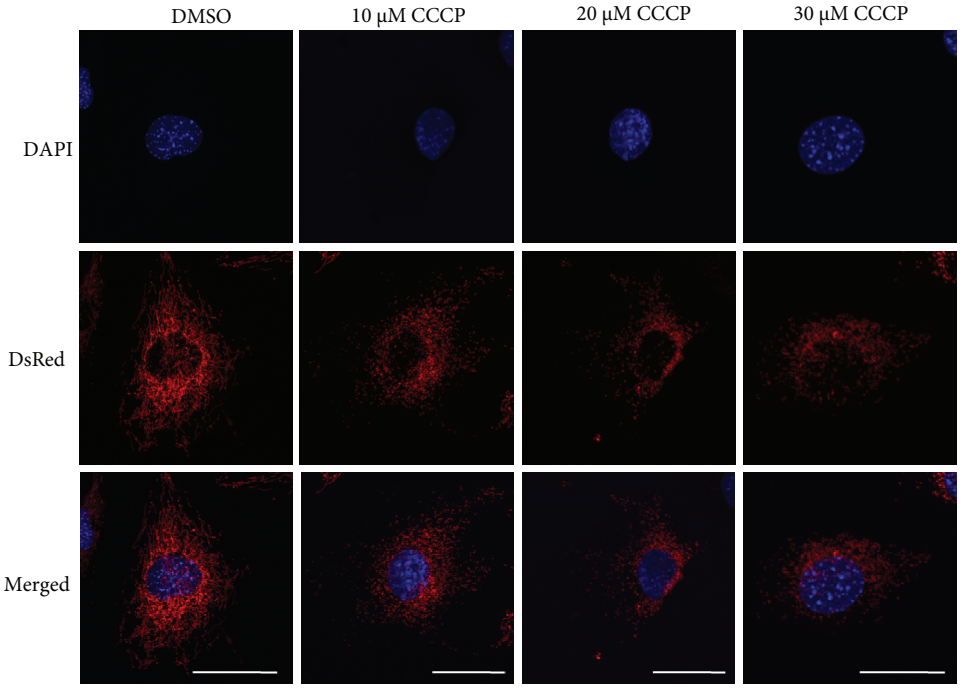

Figure 2. CCCP treatment for 6 h induces mitochondrial fragmentation. Confocal images of C2C12 skeletal muscle cells stably expressing Mito-DsRed treated with 10, 20, and 30 μM of CCCP for 6 h. Nuclei were stained with DAPI. Mitochondria are shown in red. DAPI and DsRed were excited with 405 (UV) and 561 laser lines, respectively. Scale bars = 10 μm.

3.2. CCCP increases autophagosome formation and the engulfment of mitochondria by autophagosomes

Next, we investigated whether treatment with CCCP could induce autophagy, to help understand CCCP-induced mitochondrial clearance by autophagy machinery. With this aim, we checked endogenous LC3 levels as a marker for general autophagy by biochemical and immunofluorescence analysis.

Immunofluorescence studies were performed with cells subjected to a range of conditions to monitor endogenous LC3 formation. Our confocal images demonstrated that in both the control and CCCP-treated groups, LC3 was mainly in the cytosol and had dispersed distribution. The morphology of endogenous LC3 protein showed a punctuated structure (Figure 3). In response to CCCP treatment, LC3 puncta formation was extremely abundant in the groups treated for both 3 h and 24 h (Figure 3). Furthermore, we determined LC3 lipidation as an indicator of autophagosome formation by western blot and measured the LC3-II/LC3-I ratio normalized to α-tubulin. Following CCCP treatment, the LC3-II/LC3-I ratio was increased when compared with DMSO-treated cells, and accumulation of LC3-II was significantly higher ($P < 0.001$) (Figure 4), suggesting that CCCP induces general autophagy in C2C12 Mito-DsRed cells.

We then analyzed the confocal images to establish whether autophagosomes co-localized with mitochondria. We observed a substantial co-localization of mitochondria with LC3 punctas upon CCCP-induced mitochondrial fragmentation (Figure 4). These data clearly indicate that an increase in the number of mitochondria destined for mitophagy may contribute to cell survival through the removal of dysfunctional mitochondria.

4. Discussion

Mitophagy is a dynamic process consisting of fission, fragmentation, and engulfment of mitochondria by autophagosomes (2,9). It is essential to determine the mitophagic activity of different cell lines in order to unravel the mechanism of the phenomenon. Recent studies in the field of neurodegenerative diseases, cardiovascular diseases, and diabetes are providing insight into the cellular consequences of accumulated or damaged mitochondria (3,23,24).

Here we report that C2C12 skeletal muscle cells are prone to mitochondrial fragmentation upon CCCP treatment. We observed that under basal conditions, C2C12 cells have an elongated mitochondrial network, but in response to mitochondrial uncoupler CCCP, they present massive fragmented mitochondrial morphology.

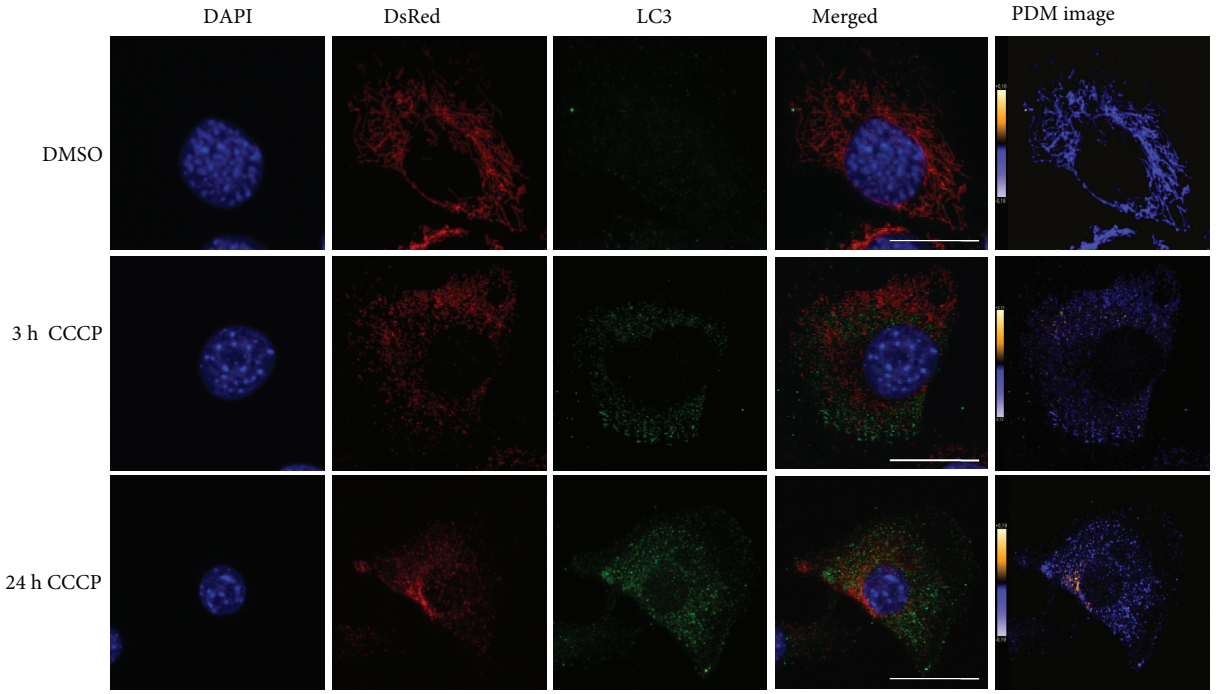

Figure 3. CCCP induces endogenous LC3 formation and increases the number of mitochondria co-localized with LC3 dots. Confocal images of C2C12 skeletal muscle cells stably expressing Mito-DsRed treated with 30 μM CCCP for 3 h and 24 h. Endogenous LC3 is shown in green. Nuclei were stained with DAPI and are shown in blue. Scale bars = 10 μm. Contrast-corrected merge RGB pictures and the Z-projection of the product of the differences from the mean (PDM) images are shown in all panels (see Section 2). Color scale shows PDM values pixel by pixel (color scales of PDM images have different maximal values; the different conditions are therefore not quantitatively comparable from these projections).

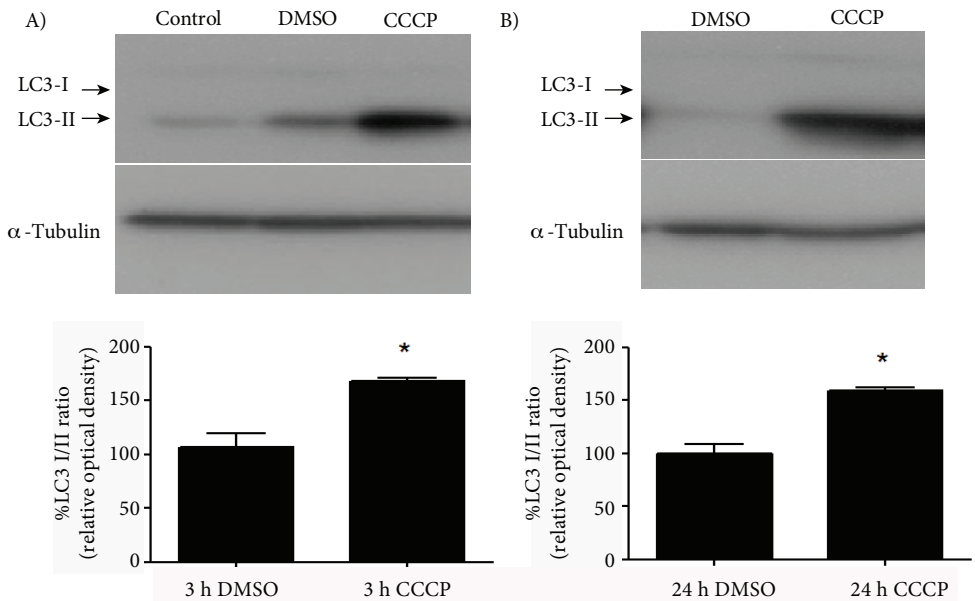

Figure 4. CCCP induces autophagosome formation. Endogenous C2C12 skeletal muscle cells were treated with DMSO or 30 μM CCCP for A) 3 h and B) 24 h (n = 3). Total cell extract was run on SDS gels and immunoblotted for endogenous LC3 and α-tubulin. Densitometry analysis of LC3-II/LC3-I is shown. Mean band density was normalized relative to α-tubulin. *: $P < 0.001$ vs. control or DMSO-treated cells.

These results are in line with data obtained from other cell lines including HEK293T, HeLa, and MEF (18,25). Indeed, deformity in the shape of mitochondria was observed after phenol exposure (26).

The link between mitochondrial dynamics and autophagy is demonstrated by the fact that fission is the event that depolarizes mitochondria, and reduced fission or an increased fusion inhibits mitophagy. On the other hand, mitochondria inside the autophagosomes loose fusion protein OPA1 and membrane potential before being targeted by autophagosomes. Therefore, it seems that mitochondrial fission and fragmentation is crucial for mitochondrial engulfment by the autophagic machinery (2,3).

Key autophagy proteins can localize to mitochondria (27,28) and several mitochondrial proteins positively regulate autophagy (29). To date, reports showing the interplay between autophagy and mitochondria suggest that autophagy machinery can specifically target dysfunctional mitochondria to remove them from the healthy mitochondrial network. In some cell lines, endogenous LC3 is present even under basal conditions without activating autophagy by nutrient deprivation or pharmacological treatment. Based on our data, basal autophagy is present also in the C2C12 skeletal muscle cell line. Our results demonstrate that CCCP directly affects autophagy induction. Confocal images also show that endogenous LC3 puncta formation increases upon mitochondrial depolarization in skeletal muscle cells. We further confirmed it by evaluating LC3 lipidation. Similarly, a study performed in HeLa cells overexpressing LC3 demonstrated that GFP-LC3 puncta formation is induced by CCCP treatment (25). It should be pointed out that the co-localization of mitochondria with LC3, which confirms the engulfment of mitochondria by the autophagy system, was extremely low in HeLa cells. Conversely, our image analysis suggests that endogenous LC3 dots co-localizing with mitochondria are abundant. This may indicate that other proteins could facilitate the removal of dysfunctional mitochondria in C2C12 skeletal muscle cells.

Based on the results of this study, we propose that CCCP induces mitochondrial fragmentation and autophagosome formation in C2C12 skeletal muscle cells, suggesting extensive removal of dysfunctional mitochondria from the whole network. These findings will enhance our understanding of the mitophagic process in C2C12 skeletal muscle cells. To date, although there are accumulating data on mitophagy regulation in different cell lines, many mechanisms of this process still need to be elucidated. Future studies will provide better insight into the pathophysiology of this pathway and, therefore, may suggest new therapeutic strategies for the treatment of diseases resulting from mitochondrial dysfunction.

References

1. Ishihara N, Jofuku A, Eura Y, Mihara K. Regulation of mitochondrial morphology by membrane potential, and DRP1-dependent division and FZO1-dependent fusion reaction in mammalian cells. Biochem Biophys Res Commun 2003; 301: 891–8.
2. Twig G, Elorza A, Molina AJ, Mohamed H, Wikstrom JD, Walzer G et al. Fission and selective fusion govern mitochondrial segregation and elimination by autophagy. EMBO J 2008; 27: 433–46.
3. Ferree A, Shirihai O. Mitochondrial dynamics: the intersection of form and function. Adv Exp Med Biol 2012; 748: 13–40.
4. Lowell BB, Shulman GI. Mitochondrial dysfunction and type 2 diabetes. Science 2005; 307: 384–7.
5. Campello S, Scorrano L. Mitochondrial shape changes: orchestrating cell pathophysiology. EMBO Rep 2010; 11: 678–84.
6. Johri A, Beal MF. Mitochondrial dysfunction in neurodegenerative diseases. J Pharmacol Exp Ther 2012; 342: 619–30.
7. Milone M, Benarroch EE. Mitochondrial dynamics: general concepts and clinical implications. Neurology 2012; 78: 1612–9.
8. Öztaş E, Topal T. A cell protective mechanism in a murine model of Parkinson's disease. Turk J Med Sci 2003;33: 295–9.
9. Kim I, Rodriguez-Enriquez S, Lemasters JJ. Selective degradation of mitochondria by mitophagy. Arch Biochem Biophys 2007; 462: 245–53.
10. Novak I. Mitophagy: a complex mechanism of mitochondrial removal. Antioxid Redox Signal 2012; 17: 794–802.
11. Youle RJ, Narendra DP. Mechanisms of mitophagy. Nat Rev Mol Cell Biol 2011; 12: 9–14.
12. Kabeya Y, Mizushima N, Ueno T, Yamamoto A, Kirisako T, Noda T et al. LC3, a mammalian homologue of yeast Apg8p, is localized in autophagosome membranes after processing. EMBO J 2000; 19: 5720–8.
13. Tanida I, Minematsu-Ikeguchi N, Ueno T, Kominami E. Lysosomal turnover, but not a cellular level, of endogenous LC3 is a marker for autophagy. Autophagy 2005; 1: 84–91.
14. Kundu M, Lindsten T, Yang CY, Wu J, Zhao F, Zhang J et al. Ulk1 plays a critical role in the autophagic clearance of mitochondria and ribosomes during reticulocyte maturation. Blood 2008; 112: 1493–502.
15. Zhang J, Ney PA. Autophagy-dependent and -independent mechanisms of mitochondrial clearance during reticulocyte maturation. Autophagy 2009; 5: 1064–5.

16. Gustafsson AB. Bnip3 as a dual regulator of mitochondrial turnover and cell death in the myocardium. Pediatr Cardiol 2011; 32: 267–74.

17. Kitada T, Asakawa S, Hattori N, Matsumine H, Yamamura Y, Minoshima S et al. Mutations in the parkin gene cause autosomal recessive juvenile parkinsonism. Nature 1998; 392: 605–8.

18. Narendra D, Tanaka A, Suen DF, Youle RJ. Parkin is recruited selectively to impaired mitochondria and promotes their autophagy. J Cell Biol 2008; 183: 795–803.

19. Kim KY, Sack MN. Parkin in the regulation of fat uptake and mitochondrial biology: emerging links in the pathophysiology of Parkinson's disease. Curr Opin Lipidol 2012; 23: 201–5.

20. Li Q, Lau A, Morris TJ, Guo L, Fordyce CB, Stanley EF. A syntaxin 1, $G\alpha_o$, and N-type calcium channel complex at a presynaptic nerve terminal: analysis by quantitative immunocolocalization. J Neurosci 2004; 24: 4070–81.

21. Rolfe DF, Brown GC. Cellular energy utilization and molecular origin of standard metabolic rate in mammals. Physiol Rev 1997; 77: 731–58.

22. Geisler S, Holmström KM, Skujat D, Fiesel FC, Rothfuss OC, Kahle PJ et al. PINK1/Parkin-mediated mitophagy is dependent on VDAC1 and p62/SQSTM1. Nat Cell Biol 2010; 12: 119–31.

23. Lim KL, Ng XH, Grace LG, Yao TP. Mitochondrial dynamics and Parkinson's disease: focus on parkin. Antioxid Redox Signal 2012; 16: 935–49.

24. Terman A, Brunk UT. Autophagy in cardiac myocyte homeostasis, aging, and pathology. Cardiovasc Res 2005; 68: 355–65.

25. Ding WX, Ni HM, Li M, Liao Y, Chen X, Stolz DB et al. Nix is critical to two distinct phases of mitophagy, reactive oxygen species-mediated autophagy induction and Parkin-ubiquitin-p62-mediated mitochondrial priming. J Biol Chem 2010; 285: 27879–90.

26. Tootian Z, Monfared AL, Fazelipour S, Shybani TM, Rouhollah F, Farhang S et al. Biochemical and structural changes of the kidney in mice exposed to phenol. Turk J Med Sci 2012; 42: 695–703.

27. Reggiori F, Shintani T, Nair U, Klionsky DJ. Atg9 cycles between mitochondria and the pre-autophagosomal structure in yeasts. Autophagy 2005; 1: 101–9.

28. Takahashi Y, Coppola D, Matsushita N, Cualing HD, Sun M, Sato Y et al. Bif-1 interacts with Beclin 1 through UVRAG and regulates autophagy and tumorigenesis. Nat Cell Biol 2007; 9: 1142–51.

29. Lee IH, Cao L, Mostoslavsky R, Lombard DB, Liu J, Bruns NE. A role for the NAD–dependent deacetylase Sirt1 in the regulation of autophagy. Proc Natl Acad Sci USA 2008; 105: 3374–9.